



Determination of halogen abundances in terrestrial and extraterrestrial samples by the analysis of noble gases produced by neutron irradiation

Lorraine Ruzié-Hamilton^{a,*}, Patricia L. Clay^a, Ray Burgess^a, Bastian Joachim^{b,c}, Christopher J. Ballentine^b, Grenville Turner^a

^a School of Earth, Atmospheric and Environmental Sciences, University of Manchester, Oxford Rd, Manchester, M13 9PL, United Kingdom

^b Department of Earth Sciences, University of Oxford, South Parks Road, Oxford, OX1 3AN, United Kingdom

^c Institute of Mineralogy and Petrography, University of Innsbruck, Innrain 52, A-6020 Innsbruck, Austria

ARTICLE INFO

Article history:

Received 13 January 2016

Received in revised form 3 May 2016

Accepted 5 May 2016

Available online 11 May 2016

Keywords:

Halogen

Neutron irradiation noble gas mass spectrometric technique

Shallowater aubrite

Scapolite standard

Barium correction

ARGUS VI mass-spectrometer

ABSTRACT

The lack of a reliable database for heavy halogens (bromine and iodine) in terrestrial and extraterrestrial samples is mainly due to the analytical challenges of determining their very low abundances (<1 ppm) in the materials of interest. The neutron irradiation noble gas mass spectrometric (NI-NGMS) technique initially developed in the 1960s is the only viable technique currently capable of determining concentrations below 1 ppb of iodine for small (<10 mg) sample sizes. We describe in detail the analytical protocols and provide a comprehensive and transparent overview of the data reduction procedures in order to fully explore the uncertainties of the technique. We demonstrate how the capabilities of modern mass spectrometers used for Ar–Ar dating, can be readily extended to incorporate halogen measurements. A new and critical assessment of the use of standards is presented based on results from multiple irradiations, including a meteorite (Shallowater aubrite), scapolite minerals introduced by Kendrick (2012) and a novel internal calibration method based on using barium.

© 2016 The Authors. Published by Elsevier B.V. This is an open access article under the CC BY license (<http://creativecommons.org/licenses/by/4.0/>).

1. Introduction

Halogens are present as minor and trace elements in most geological samples. Studies of halogens have been applied to crustal and ore-forming fluids (e.g.; Böhle and Irwin, 1992a,b; Turner and Bannon, 1992; Ballentine et al., 2002; Kendrick and Burnard, 2013) and more recently, the determination of heavy halogens (bromine and iodine) in mantle-derived samples has provided important constraints on the origin and the recycling of the major volatile elements in the Earth (Burgess et al., 2002, 2009; Sumino et al., 2010; Kendrick et al., 2011, 2012a,b, 2013a,b). However, low concentrations of halogens in the materials of interest, together with the lack of available techniques for their low level detection, means that reliable abundance data are relatively sparse compared to other volatile elements. Whilst the electron microprobe (EMP) can determine chlorine and fluorine abundances down to levels of 0.01 wt.%, bromine and iodine abundances are <1 ppm in most minerals and rocks. Chlorine and bromine can be determined by instrumental neutron activation analysis (INAA) but require >100 mg-size samples (e.g. Heinrich et al., 1993). Similarly, ion chromatography analysis requires crush-leaching of gram-sized samples to extract halogens

(e.g. Bottrell and Yardley, 1988). Recently, Heinrich et al. (2003) assessed the potential of Br and Cl quantification by LA-ICP-MS. However the halogens tend to have low ionisation efficiencies leading to relatively low sensitivity. Using LA-ICP-MS for scapolite minerals, Hammerli et al. (2013) determined detection limits of about 8 ppm Br and >500 ppm for Cl. Time-of-Flight Secondary Ion Mass Spectrometry (TOF-SIMS) has been used with detection limits of 10 ppm for F and Cl (Joachim et al., 2015) and SIMS has attained limits of 0.6 ppm for Br and 0.035 ppm for I (Kusebauch et al., 2015).

An alternative technique for halogen determination is based upon extension of the ⁴⁰Ar–³⁹Ar technique (Merrihue, 1965; Turner, 1965; Turner et al., 1971; Turner and Bannon, 1992; Böhle and Irwin, 1992a, b; Irwin and Roedder, 1995). Although fairly routinely used for Cl, this technique has only recently become more widely adopted for Br and I following a revival in the 2000s by the Manchester Isotope Geochemistry and Cosmochemistry group (Johnson et al., 2000; Kendrick et al., 2001; Burgess et al., 2002). Kendrick (2012) summarises in detail the basic concepts of the neutron-irradiation noble gas technique. The author suggested the use of the mineral scapolite as a standard for halogen determinations to replace the existing meteorite standards (Shallowater or Bjurböle). Subsequently, Kendrick et al. (2013a) have revised the halogen values of the scapolite standards, reducing them by 22% and 27% for Br and I, respectively. This correction has been

* Corresponding author.

independently confirmed for Br by Hammerli et al. (2014) in scapolites, but no external standards or techniques have been used to verify I concentrations.

The introduction of scapolite standards has an impact on the way previous workers have reduced their data to estimate the halogen abundances in natural samples. We discuss the implications by describing different approaches to reduce the data. We compare results from five different irradiations using two different reactors. We introduce an alternative halogen standardisation method based on the barium content (when known independently) of irradiated samples, referred to from hereon as a barium calibration. Finally, the results obtained from the Shallowater meteorite and the barium correction are used to refine the I/Cl values of BB2/SP and BB1 scapolite standards of Kendrick et al. (2013a) and reduce their 2 σ -errors from 23% (BB2/SP) and 15% (BB1) to 14% and 10%, respectively.

2. Method of investigation

2.1. General principle

The ^{40}Ar – ^{39}Ar technique is widely used for geological dating and can be adapted for a range of elements forming noble gas isotopes during (n, p), (n, α), (n, γ , β) or neutron-induced fission reactions (Table 1; Turner, 1965). During neutron irradiation $^{39}\text{K}(\text{n}, \text{p})^{39}\text{Ar}$ and $^{40}\text{Ca}(\text{n}, \alpha)^{37}\text{Ar}$ reactions are activated only by fast neutrons i.e. having energy >1 MeV. In contrast, halogen-derived noble gas isotopes are produced by low energy thermal neutrons (10^{-11} – 2.5×10^{-8} MeV) and epithermal neutrons (2.5×10^{-8} –1 MeV). Halogen determinations are accessible through (n, γ , β) reactions forming noble gas isotopes (Fig. 1; Table 1) in amounts readily detected by noble gas mass spectrometers.

Integrated neutron fluences are typically in the range 10^{18} – 10^{19} n·cm $^{-2}$ with most halogen absorption reactions involving thermal and epithermal neutrons (Fig. 2) leading to conversion factors between 10^{-6} and 10^{-4} of the parent halogen atoms.

Using the approach of Chilian et al. (2006) for INAA, upon irradiating a sample containing an amount m (grams) of an element, then the quantity of a given nuclide ^iX (moles) produced by a (n, γ , β) reaction is given by:

$$^i\text{X} = \frac{m}{M_{\text{at}}} \cdot \theta \cdot \sigma_{\text{th}} \cdot Y \cdot \varphi_{\text{th}} \cdot \frac{Q_0}{f} \quad (1)$$

where M_{at} is the atomic mass, θ is the isotopic abundance; Y is the fractional yield for branched isotope decay; σ_{th} is the thermal neutron absorption cross section (2200 ms^{-1}); $Q_0 = \sigma_{\text{epi}}/\sigma_{\text{th}}$ is the ratio of resonance integral to thermal neutron cross-section, $f = \varphi_{\text{th}} / \varphi_{\text{epi}}$ with φ_{th} and φ_{epi} being the thermal and epithermal neutron fluences, respectively (Table 2). The parameter f is usually not known *a priori* and will vary with reactor and irradiation position; however it can be determined experimentally from standards. The proportion of

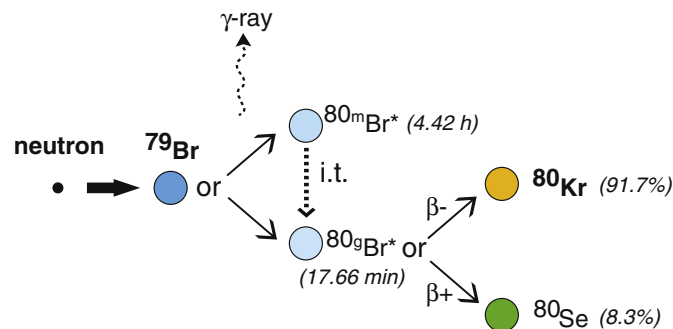


Fig. 1. Schematic example of neutron irradiation for ^{79}Br . ^{79}Br can be either activated to radioactive $^{80\text{m}}\text{Br}^*$ or $^{80\text{g}}\text{Br}^*$ (m = metastable state and g = ground state). $^{80\text{m}}\text{Br}$ decays to $^{80\text{g}}\text{Br}$ during an isomeric transition (i.t.), which then decays to ^{80}Se (8.3%) or ^{80}Kr (91.7%).

epithermal neutron-induced isotope production can be estimated as $Q_0 / (Q_0 + f)$, or expressed by the F-factor as:

$$F = \frac{Q_0 + f}{f} \quad (2)$$

As an example, our irradiation MN2014b carried-out in the GRICIT Facility at the TRIGA reactor Oregon gave $f = 11.3 \pm 2.3$ (Table 2), with $^{80}\text{Kr}_0 = 11.9 \pm 0.3$ and $^{80}\text{Kr}_0 = 24.9 \pm 0.7$ (Table 2), this indicates that 51% of the $^{80}\text{Kr}_{\text{Br}}$ and 69% $^{128}\text{Xe}_1$ is formed by epithermal neutron absorption.

In contrast, nucleogenic production of ^{38}Ar from ^{37}Cl has a relatively low Q_0 value ($= 0.7 \pm 0.1$) and therefore is used to monitor the thermal neutron fluence. Eq. (1) can be useful for irradiation planning if the epithermal/thermal fluence ratio of a reactor irradiation position has been previously characterised and remains relatively constant over time. However, Eq. (1) does not include the effects of neutron self-shielding on isotope production. Analytical formulae for correcting self-shielding effects in cylindrical samples (appropriate for samples irradiated in silica glass tubes) are given by Chilian et al. (2006, 2008, 2010). The effects of self-shielding are likely to be negligible for most samples used in ^{40}Ar – ^{39}Ar irradiations, because of their relatively low mass (usually <0.01 g) and the low concentrations of target elements (for halogens typically at ppb–ppm levels). Self-shielding effects should be considered when irradiating samples with high concentrations of halogens (e.g. halogen salts), in which self-shielding by epithermal neutrons at resonance peaks could be severe (Chilian et al., 2006). For example, using the method of Chilian et al. (2006), it is estimated that epithermal self-shielding of a 1g cylindrical (radius = 1 cm; height = 2 cm) sample of iodide salt (NaI or KI) could lead to an erroneous underestimate of I abundance from $^{128}\text{Xe}_1$ of up to 38%.

The halogen abundances in samples can be evaluated either from the derived neutron fluence, or from standards of known parent element

Table 1
Summary of the neutron-induced reactions forming noble gas isotopes used in this study. Thermal neutron cross-sections are given for neutrons with energy of 0.0253 eV. Barn = 10^{-24} cm^2 .

Parent	Isotopic abundance	Noble gas product	Reactions	Neutron involved	Thermal cross section (barns)	Resonance integral (barns)	Yield
^{37}Cl	0.2424	$^{38}\text{Ar}_{\text{Cl}}$	$^{37}\text{Cl}(\text{n}, \gamma)^{38}\text{Cl}(\beta)^{38}\text{Ar}$	Thermal	0.433 ± 0.006^a	0.30 ± -0.04^a	1
^{39}K	0.9326	$^{39}\text{Ar}_{\text{K}}$	$^{39}\text{K}(\text{n}, \text{p})^{39}\text{Ar}$	Fast	2.1 ± 0.1^a	1.1 ± 0.1^a	1
^{40}Ca	0.9694	$^{37}\text{Ar}_{\text{Ca}}$	$^{37}\text{Ca}(\text{n}, \alpha)^{37}\text{Ar}$	Fast	0.43 ± 0.02^a	0.22 ± 0.02^a	1
^{79}Br	0.5069	$^{80}\text{Kr}_{\text{Br}}$	$^{79}\text{Br}(\text{n}, \gamma)^{80}\text{Br}(\beta)^{80}\text{Kr}$	Thermal + epithermal	10.89 ± 0.05^b	129.6 ± 3.0^b	0.917
^{81}Br	0.4931	$^{82}\text{Kr}_{\text{Br}}$	$^{81}\text{Br}(\text{n}, \gamma)^{82}\text{Br}(\beta)^{82}\text{Kr}$	Thermal + epithermal	2.36 ± 0.03^b	46.3 ± 1.7^b	1
^{127}I	1.0000	$^{128}\text{Xe}_{\text{I}}$	$^{127}\text{I}(\text{n}, \gamma)^{128}\text{I}(\beta)^{128}\text{Xe}$	Thermal + epithermal	6.16 ± 0.04^b	153.4 ± 3.9^b	0.94
^{130}Ba	0.00106	$^{131}\text{Xe}_{\text{Ba}}$	$^{130}\text{Ba}(\text{n}, \gamma)^{131}\text{Ba}(\beta)^{131}\text{Xe}$	Thermal + epithermal	7.75 ± 0.34^c	197.3 ± 10^c	1

^a Data source: Pritychenko and Mughabghab (2012).

^b See Supplementary data-Tables C1–C3–3–.

^c Dauenhauer and Krane (2012) and see section 4.3.

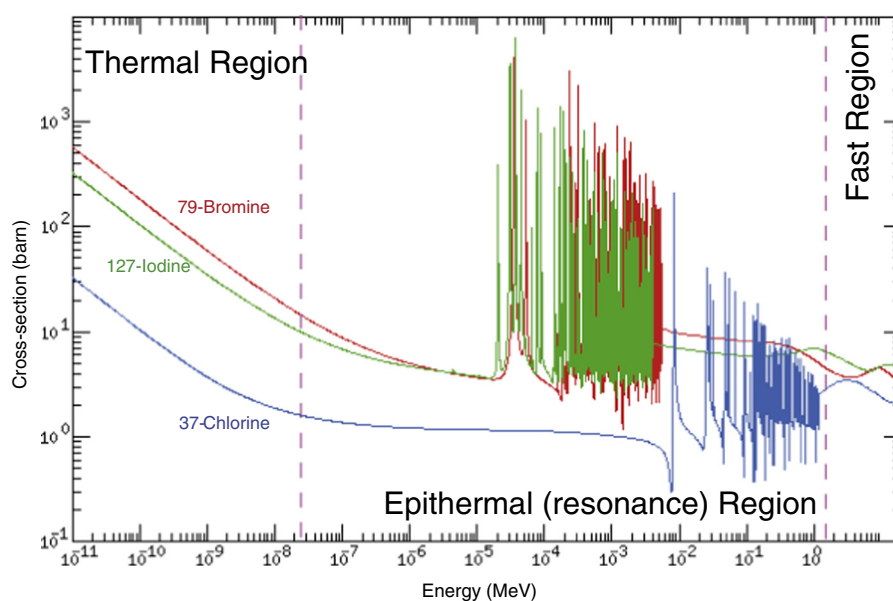


Fig. 2. Variation of absorption cross sections with neutron energy for relevant isotopes of Cl, Br and I. The neutron flux is comprised of thermal (φ_{th}), epithermal (also referred to as resonance neutrons) (φ_{epi}) and the fast neutron (φ_{fast}) components. Nucleogenic isotope production is dominated by thermal neutron absorption, however strong resonances at higher energy mean that it is essential to use standards to estimate the irradiation parameters (modified from <http://atom.kaeri.re.kr>).

composition. We compare these methods and discuss implications in Section 4.

2.2. Samples and neutron irradiation

Irradiation standards used in this study include the hornblende age standard Hb3gr (Turner et al., 1971), three scapolite minerals (BB1, SP2 and BB2) previously described by Kendrick (2012) and the Shallowater aubrite meteorite, a commonly used I-Xe standard (Gilmour et al., 2006).

Prior to irradiation, each sample and monitor were wrapped in aluminum foil. They were placed in a quartz tube, evacuated and sealed to a maximum length of 6.5 cm using a flame. Hb3gr hornblendes were positioned in the bottom, middle and top of each quartz tube. Shallowater was positioned in the middle of the tube. Scapolite standards were placed at the bottom and top of each tube. This procedure has been used in five irradiations carried-out between 2012 and 2014 so that

results can be directly compared. Sample batches MN2012b, MN2012f (both in 2012) and MN2013 (in 2013) were irradiated in the RODEO facility (High Flux Reactor, Petten, Netherlands) with a constant rotation during irradiation. In 2014, irradiations were carried-out in ICIT (MN2014a) and GRICIT (MN2014b) facilities of the TRIGA Reactor, Oregon State University (OSU). As the halogen-derived noble gas isotopes are produced by low energy thermal neutrons and epithermal neutrons, the irradiation cans were not Cd-shielded. The Petten irradiations were each irradiated continuously for 24 h duration. At OSU samples were irradiated for a few hour intervals each day over several weeks to give a total irradiation time of 278 and 205 h for MN2014a and MN2014b respectively. All the irradiation details are provided in Table 2.

2.3. Noble gas extraction and mass spectrometry

Noble gas isotopic measurements were made using either MS1, a custom built single focusing magnetic sector mass spectrometer

Table 2

Details of the nuclear irradiations carried-out in the Petten high fluence reactor in 2012 and 2013 and Oregon State University reactor in 2014 (ICIT and GRICIT).

Irradiation	MN2012b	MN2012f	MN2013	MN2014a	MN2014b
Reactor	Petten	Petten	Petten	OSU-ICIT	OSU-GRICIT
Date	16/05/2012	24/07/2012	26/07/2013	30/04 to 01/08-2014	22/04 to 01/07-2014
Duration	24 h	24 h	24 h	278.4 h	205.1 h
# of Hb3gr	33	10	11	16	12
J^a	0.00641 ± 0.00013	0.00626 ± 0.00011	0.00631 ± 0.00009	0.078 ± 0.002	0.017512 ± 0.0003
Thermal ^b	$(6.40 \pm 0.06) \times 10^{18}$	$(6.34 \pm 0.09) \times 10^{18}$	$(6.17 \pm 0.03) \times 10^{18}$	$(6.47 \pm 0.23) \times 10^{18}$	$(2.48 \pm 0.13) \times 10^{18}$
Epithermal ^c	$(1.59 \pm 0.16) \times 10^{17}$	$(1.38 \pm 0.19) \times 10^{17}$	$(1.59 \pm 0.35) \times 10^{17}$	$(9.49 \pm 0.01) \times 10^{17}$	$(2.19 \pm 0.05) \times 10^{17}$
f^d	38.1 ± 3.8	39.4 ± 6.4	33.1 ± 6.6	6.8 ± 0.2	11.3 ± 2.3
Alpha ^e	0.49 ± 0.03	0.50 ± 0.03	0.49 ± 0.02	0.90 ± 0.02	0.53 ± 0.05
Beta ^f	9.5 ± 0.1	9.8 ± 0.5	9.3 ± 0.2	0.78 ± 0.02	1.34 ± 0.07

^a Calculated from Eq. (A.17 - Supp. Data).

^b Calculated from Eq. (A.21 - Supp. Data) ($n \cdot cm^{-2}$).

^c The epithermal fluence ($n \cdot cm^{-2}$) has been calculated using Shallowater (Brazzle et al., 1999).

^d $f = \varphi_{th} / \varphi_{epi}$.

^e Calculated from Eq. (A.18 - Supp. Data) (Turner, 1972).

^f Calculated from Eq. (A.19 - Supp. Data) (Kelley et al., 1986).

Table 3

Mass spectrometer ion source and noble gas characteristics of the MS1 and ARGUS VI mass spectrometers. Sensitivities and isotope ratios are calculated over a month long-period (10).

	MS1	ARGUS VI
Acceleration voltage (kV)	3	2.5
Trap current (microA)	250	230
Electron energy (eV)	110	87.40
Volume MS (cm ³)	740	680
Argon sensitivity (cm ³ /A)	1.67×10^{-12}	1.24×10^{-12}
Krypton sensitivity (cm ³ /A)	2.18×10^{-12}	7.73×10^{-13}
Xenon sensitivity (cm ³ /A)	1.84×10^{-12}	9.45×10^{-13}
⁴⁰ Ar/ ³⁶ Ar (= 298.56 ± 0.54) _{air}	295.98 ± 1.81	299.54 ± 0.78
⁸² Kr/ ⁸⁴ Kr (= 0.20217 ± 0.00004) _{air}	0.20331 ± 0.00255	0.20619 ± 0.00891
¹³² Xe/ ¹²⁹ Xe (= 1.01) _{air}	0.99 ± 0.06	1.01 ± 0.05

(15 cm, 90° geometry) that has been in operation for nearly 50 years,¹ or a ThermoFisher Scientific ARGUS VI mass spectrometer, one of the latest generation of multi-collector instruments (Table 3).

2.3.1. MS1

The MS1 mass spectrometer sensitivity is optimised for the measurement of low abundance Xe isotopes. It has a Baur-Signer source and a detector slit configured for high transmission (sensitivity of 3×10^{-4} A/Torr ⁴⁰Ar). The ion beams are detected using either a Faraday cup capable of measuring 10^{-6} – 10^{-15} A using a 10^{11} Ohm amplifier or a continuous dynode channeltron measuring 10^{-13} – 10^{-19} A.

Noble gases are extracted from samples using a tantalum resistance furnace operating over a temperature range of 400–1800 °C. Samples are loaded via a conventional Pyrex glass “Christmas Tree” holding up to 12 samples. Prior to sample analyses, the furnace is outgassed several times at 1750 °C for 30 min and blanks are determined by heating the empty furnace to each target temperature steps (600 °C, 1400 °C, 1600 °C and 1700 °C). Samples are dropped into the furnace with an iron slug operated by an external hand magnet. Each heating step is for 30 min during which noble gases are purified of active gases using a getter (SEAS NP10) at 400 °C. Once extracted, the noble gases are transferred to the inlet manifold of the mass spectrometer where the noble gases (Ar, Kr, Xe) are gettered for a further 5 min (SEAS ST172) at 250 °C. Argon, Kr and Xe are transferred onto a charcoal cold-finger cooled with liquid nitrogen for 5 min in order to concentrate them into the mass spectrometer inlet manifold. The charcoal finger is then warmed for 5 min to 50 °C and the noble gases expanded into the mass spectrometer. Isotopic analyses are made statically with Ar, Kr and Xe isotopes measured sequentially seven times (50 min total duration). Argon isotopes are measured on the Faraday collector whilst the less abundant Kr and Xe isotopes are measured using the channeltron. Each heating, purification and isotopic analysis step takes a total duration of approximately 1.5 h. Aliquots of air are analysed daily using a similar procedure to the samples in order to check the sensitivity and mass discrimination of the MS1 mass spectrometer.

2.3.2. ARGUS VI

The Thermo Fisher Scientific ARGUS VI is a static vacuum mass spectrometer with 13 cm, 90° extended geometry ion optics principally designed for the multi-collection of Ar isotopes in neutron-irradiated samples (*m/z* 36, 37, 38, 39 and 40). The collector array consists of five Faradays (in positions H2, H1, Axial, L1 and L2) and a low mass compact discrete dynode (CDD) ion counting multiplier. This design enables simultaneous collection of ⁴⁰Ar on H2 or H1; ³⁹Ar on H1 or Ax; ³⁸Ar on Axial or L1; ³⁷Ar on L1 or L2 and ³⁶Ar on L2 or CDD. Coupled to its low volume (680 cm³), the instrument utilizes a X- and Z-focused Nier type bright source giving sensitivities in excess of 1×10^{-3} A/Torr ⁴⁰Ar at 200 μA trap current and 4.5 kV acceleration voltage.

In order to measure the xenon isotopes, the accelerating voltage is reduced to 2.5 kV and the filament trap current increased to 230 μA. The ion source is optimised for sequential analysis of Ar, Kr and Xe isotopes. The sensitivities are: 1.24×10^{-12} cm³ STP Ar/A, 7.73×10^{-13} cm³ STP Kr/A and 9.45×10^{-13} cm³ STP Xe/A. The gases are extracted using a 10.6 μm wavelength CO₂ laser (CETAC Fusion CO₂) with a 3 mm beam diameter. The 55 W output CO₂ laser allows for the controlled stepped heating of samples. Samples are loaded into 3 mm diameter holes drilled into an Al sample holder. The view-port window and cover slip are made of ZnS. For Hb3Gr hornblende, noble gases are extracted in three laser heating steps of 25 s each: 1) 0.5% to 3% of the laser power; 2) 3% to 6%; and 3) 7% to 9%. The scapolite standards are heated in a single step by slowly increasing the laser power from 6% to 10% over 180 s. For the Shallowater meteorite, at least eight individual heating steps are used from 0.5% (30 s) to 9% (30 s). Purification time on a hot getter (NP10) is 4 min, followed by five minute transfer onto a liquid nitrogen cooled charcoal finger. Following transfer, the charcoal finger is warmed for 5 min to 60 °C to release noble gases. The purified unseparated noble gases are expanded into the mass spectrometer. Introducing Ar, Kr and Xe at the same time reduces any elemental fractionation between Kr and Ar associated with their sequential release by heating the charcoal finger. Xenon isotopes (128–136) are detected first by magnetic switching of the peaks on the CDD. Argon data are collected using multicollection with the five Faraday cups. Finally, krypton isotopes (⁸⁶Kr, ⁸⁴Kr, ⁸²Kr and ⁸⁰Kr) are collected in a single step on H2 (⁸⁶Kr), H1 (⁸⁴Kr), AX (⁸²Kr) and L1 (⁸⁰Kr). The multicollection of krypton isotopes is achieved by applying a small voltage to the entrance of each Faraday cup (Thermo Fisher Scientific, Deflection Plate Technology). The isotopic analyses of nine cycles takes approximately 20 min, at the end of which isotope abundances are determined by regression to inlet time.

3. Determining abundances of K, Ca and Cl

All measurements made on samples and irradiation standards are subject to the corrections outlined below. Argon data are corrected in order of instrumental background, mass discrimination, radioactive decay of ³⁷Ar_{Ca} and ³⁹Ar_K, and neutron interference reactions. These are conventional corrections applied for ⁴⁰Ar–³⁹Ar age dating (e.g. McDougall and Harrison, 1999) and a summary is provided for completeness in Supplementary section A. The irradiation parameters (*J*, *α* and *β*) are calculated using Hb3Gr monitor. The hornblende Hb3gr was chosen as a monitor by Turner et al. (1971) due to its homogeneity in terms of composition and age. For this study we used the value determined by Schwarz and Trierloff (2007) of 1074.9 ± 3.5 Ma.

K, Ca and Cl (moles) are determined using Eqs. (3) to (5). Further details are provided in the Supplementary section A.

$$K = (3.66 \pm 0.03) \cdot \frac{[^{39}\text{Ar}]}{J} \quad (3)$$

$$\text{Ca} = (3.57 \pm 0.03) \cdot \frac{[^{37}\text{Ar}]}{J \cdot \alpha} \quad (4)$$

$$\text{Cl} = (4.04 \pm 0.04) \cdot \frac{[^{38}\text{Ar}]}{J \cdot \beta} \quad (5)$$

4. Epithermal neutron production and Br, I and Ba abundances

Earlier studies showed that that absorption of epithermal neutrons at resonance peaks in the cross-sections of ⁷⁹Br and ¹²⁷I account for about 30% of ⁸⁰Kr_{Br} and 40–50% of ¹²⁸Xe_I produced during irradiation (Böhlke and Irwin, 1992b; Johnson et al., 2000; Kendrick, 2012). Therefore the noble gas/parent halogen production ratios require calibration by analysing a standard with known concentrations of Br and I. Initially,

¹ <http://www.seaes.manchester.ac.uk/our-research/research-areas/pes/isotope-geochemistry-and-cosmochemistry/facilities/noble-gas-labs/ms-1/>.

Turner (1965) used potassium iodide and potassium bromide to measure the integrated neutron fluence. Both Kr and Xe from these salts were measured by isotope dilution in that work. This approach was used until the end of the 1980s. However, self-shielding processes will almost certainly have impacted on the correction factors, as discussed earlier. To circumvent this effect a meteorite standard was introduced to calibrate the I-Xe system.

In the following section, we consider three different approaches to monitor noble gas isotope production from epithermal neutrons: the Shallowater aubrite (Johnson et al., 2000), scapolite minerals (Kendrick, 2012) and a novel technique based on barium in samples. In order to test the different corrections we use a set of six Mid-Ocean Ridge Basalt (MORB) samples irradiated in MN2012b that were analysed on both the ARGUS VI and MS1 mass spectrometers. Details about these samples can be found in the Supplementary data section B.

Noble gases are corrected for neutron-induced fission of ^{235}U (Kr and Xe; Supplementary data section A.8) and atmospheric contamination using natural isotopes least affected by the irradiation procedure (i.e. ^{36}Ar , ^{84}Kr and ^{130}Xe).

4.1. Meteorite standards

The Shallowater (SW; aubrite) and Bjurböle (BJU; L/LL4 ordinary chondrite) meteorites were adopted as iodine standards (e.g. Johnson et al., 2000) because they are commonly used in I-Xe dating. Determining the $^{128}\text{Xe}/^{129}\text{Xe}$ in the irradiated meteorite and comparing the result with the initial $^{129}\text{Xe}/^{129}\text{I}$ ($^{129}\text{Xe}/^{129}\text{I}_{\text{SW}} = 1.125 \pm 0.012 \times 10^{-4}$ – Hohenberg, 1967; Turner, 1965; $^{129}\text{Xe}/^{129}\text{I}_{\text{SW}} = 1.072 \pm 0.029 \times 10^{-4}$ – Brazzle et al., 1999) and $^{129}\text{Xe}/^{129}\text{I}_{\text{BJU}} = 1.095 \pm 0.029 \times 10^{-4}$ – Hohenberg and Kennedy, 1981), is used to quantify the $^{128}\text{Xe}_\text{I}$ produced during irradiation.

First the thermal neutron production ratio is calculated as:

$$\frac{^{128}\text{Xe}_\text{I}}{\text{I}} = \varphi_\text{th} \cdot \sigma_\text{th} \cdot Y_{128\text{I}} \cdot \theta_{128\text{I}} \quad (6)$$

where φ_th is determined from Hb3gr (Eq. A.21), using $Y_{128\text{I}} = 0.94$, $\sigma_\text{th} = 6.16 \pm 0.04$ b (Supplementary data -Table C.1) and $\theta_{128\text{I}} = 1$. The total (thermal + epithermal) production ratio is calculated using the measured $^{128}\text{Xe}/^{129}\text{Xe}$ ratio and the initial ($^{129}\text{Xe}/\text{I}$)₀ in the meteorite standard according to,

$$\frac{^{128}\text{Xe}}{\text{I}} = \left(\frac{^{129}\text{Xe}}{\text{I}} \right)_0 \cdot \left(\frac{^{128}\text{Xe}}{^{129}\text{Xe}} \right)_\text{measured} \quad (7)$$

By dividing Eq. (6) by Eq. (7), we can estimate the iodine factor (F_I). This factor is used to determine the amount of ^{128}Xe produced from ^{127}I by epithermal neutrons.

Conventionally the $^{128}\text{Xe}/^{129}\text{Xe}$ ratio is obtained from the meteorite standard via the slope of concordant heating steps using an I-Xe isotope correlation diagram. The data from the meteorite typically shows discordant low temperature steps and concordant data for high temperature steps (e.g. Hohenberg, 1967 – Fig. 1).

Stepped heating of Shallowater was carried-out on the ARGUS VI using the CO_2 fusion laser (Fig. 3). As the methodology for xenon measurements is new on the ARGUS VI mass spectrometer, we compared our analyses of Shallowater samples from the same irradiation using the RELAX mass spectrometer (S. Crowther - pers. comm.). RELAX (Refrigerator Enhanced Laser Analyser for Xenon) is an ultrasensitive resonance ionisation time-of flight mass spectrometer with micro-channel plate detectors designed for the analyses of very small amounts of xenon (Gilmour et al., 1991, 1994; Crowther et al., 2008). The lower sensitivity of the ARGUS VI compared to RELAX for Xe results in fewer temperature steps despite larger sample sizes (2.5 mg versus 0.5 mg). However, for the same irradiation MN2014a (OSU), the $^{129}\text{Xe}/^{128}\text{Xe}$ ratios are in excellent agreement (0.646 ± 0.042 – ARGUS VI and 0.654 ± 0.014 (RELAX). For the Petten reactor, we can only compare Shallowater data for MN2013 (ARGUS VI) to a previous irradiation MN2012f (RELAX) however the $^{129}\text{Xe}/^{128}\text{Xe}$ value should be relatively constant over time for the same irradiation position within a reactor. Using the ARGUS VI we obtained ($^{129}\text{Xe}/^{128}\text{Xe}$)_{MN2013} of 1.83 ± 0.15 (1σ) for Shallowater and using RELAX we obtained a ($^{129}\text{Xe}/^{128}\text{Xe}$)_{MN2012f} ratio of 1.869 ± 0.004 (1σ). To calculate the production of $^{80}\text{Kr}_\text{Br}$ by epithermal neutrons, the epithermal fluence is calculated using the $^{128}\text{Xe}/\text{I}$ value obtained from Shallowater:

$$\varphi_\text{epi} = \frac{\left(\left[\frac{^{128}\text{Xe}/\text{I}}{Y} \right] - [\varphi_\text{th} \cdot \sigma_\text{th}] \right)}{\sigma_\text{epi}} \quad (8)$$

The amount of ^{80}Kr produced by ^{79}Br is given by,

$$^{80}\text{Kr}_\text{Br} = ^{79}\text{Br} \cdot Y_{79\text{Br}} \cdot \theta_{79\text{Br}} \cdot (\varphi_\text{th} \cdot \sigma_\text{th} + \varphi_\text{epi} \cdot \sigma_\text{epi}) \quad (9)$$

with σ_th and σ_ep given in Table 1 and Supplementary data – Tables C.1 and C.3. The correction factors ($F_{79\text{Br}}$, $F_{81\text{Br}}$, $F_{127\text{I}}$ and $F_{131\text{Ba}}$) calculated using this method are shown in the Table 4 for all irradiations.

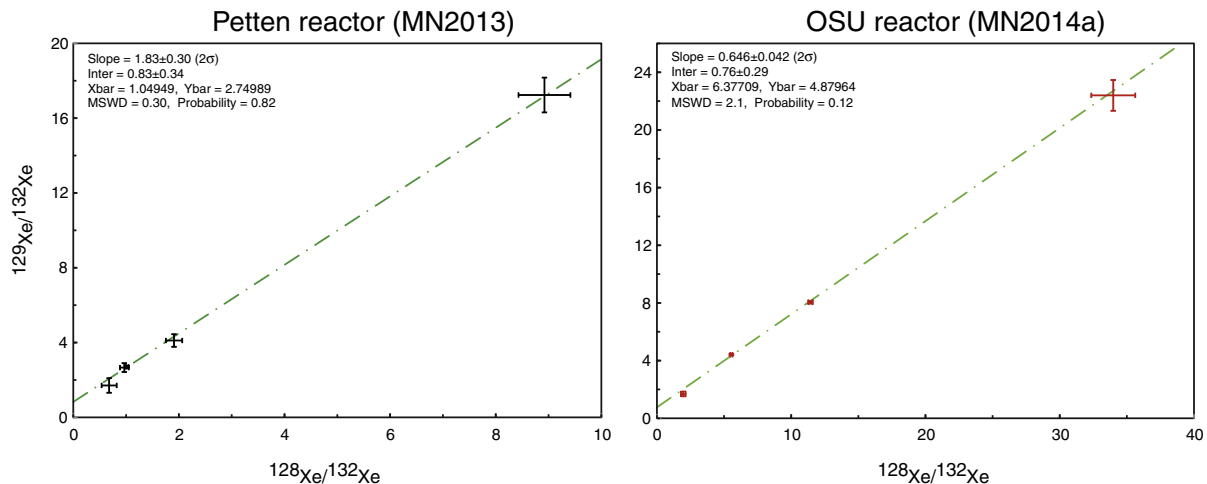


Fig. 3. Example of xenon isotope step heating measurements on ARGUS VI for Shallowater meteorite. Results are shown for the OSU reactor (MN2014a) and for the Petten reactor (MN2013). The regressions were calculated using Isoplot 4.1 (Ludwig, 2012). The lower error on the slope for the OSU irradiated sample is explained by the much larger sample size used.

Table 4
Correction factors (F-values) for Br, I and Ba. These were calculated using the epithermal fluence estimated from Shallowater (SW) standards. SW values were obtained from a step at 1400 °C using a furnace, and SW* are the slopes of the $^{129}\text{Xe}/^{132}\text{Xe}$ – $^{128}\text{Xe}/^{132}\text{Xe}$ correlations obtained from multiple heating steps.

Irradiation	MN2012b	MN2012f	MN2013		MN2014a		MN2014b
Reactor	Petten				OSU-ICIT		OSU-GRICIT
Method	SW	SW*	SW	SW*	SW	SW*	SW*
MS	MS1	RELAX	MS1	ARGUS	RELAX	ARGUS	ARGUS
# samples	4	1	5	1	1	1	2
$F(^{79}\text{Br})$	1.30 ± 0.03	1.25 ± 0.02	1.42 ± 0.08	1.31 ± 0.01	2.60 ± 0.03	2.61 ± 0.03	2.05 ± 0.02
$F(^{81}\text{Br})$	1.49 ± 0.05	1.42 ± 0.02	1.69 ± 0.13	1.50 ± 0.01	3.64 ± 0.02	3.65 ± 0.02	2.73 ± 0.04
$F(^{127}\text{I})$	1.62 ± 0.06	1.53 ± 0.06	1.87 ± 0.17	1.64 ± 0.14	4.36 ± 0.16	4.36 ± 0.19	3.20 ± 0.05
$F(^{130}\text{Ba})$	1.63 ± 0.07	1.54 ± 0.06	1.82 ± 0.14	1.65 ± 0.05	4.43 ± 0.08	4.44 ± 0.08	3.25 ± 0.05

4.2. Scapolite standards

Kendrick (2012) introduced scapolite (SP, BB2 and BB1) as a potential new standard for the analysis of Cl, Br and I. Subsequently, Kendrick et al. (2013a) irradiated the scapolite standards with a high thermal fluence making the correction for epithermal production negligible (<2%). Following the recommendation of Kendrick et al. (2013a) the revised halogen abundances of the scapolite standard values are given in Table 5.

In order to calculate halogen abundances in samples the halogen ratios measured in the scapolite minerals are equated to the halogen-derived noble gases formed during irradiation. The notations π and ω were proposed by Kendrick (2012), analogous to α and β constants (Eqs. A.18 and A.19– Supplementary data):

$$\frac{\text{Cl}}{\text{Br}} = \pi \frac{{}^{38}\text{Ar}_{\text{Cl}}}{{}^{80}\text{Kr}_{\text{Br}}} \quad (10)$$

$$\frac{\text{Cl}}{\text{I}} = \omega \frac{{}^{38}\text{Ar}_{\text{Cl}}}{{}^{128}\text{Xe}_{\text{I}}} \quad (11)$$

The results for π and ω are presented in Table 6. In order to obtain a comparable set of corrections using different approaches, we apply a common notation of correction F-factors-as follows. The production of noble gas proxy isotopes from thermal neutrons is given by:

$$\begin{aligned} \frac{{}^{80}\text{Kr}_{\text{Br}}}{{}^{38}\text{Ar}_{\text{Cl}}} &= \frac{\text{Br} \cdot \varphi_{\text{th}} \cdot \sigma_{79\text{Br}} \cdot Y_{79\text{Br}} \cdot \theta_{79\text{Br}}}{\text{Cl} \cdot \varphi_{\text{th}} \cdot \sigma_{37\text{Cl}} \cdot Y_{37\text{Cl}} \cdot \theta_{37\text{Cl}}} \\ &= \frac{\text{Br}}{\text{Cl}} \times 48.228(\pm 0.312)(\text{molar ratio}) \end{aligned} \quad (12)$$

Therefore the Br/Cl ratio in the sample produced by thermal neutrons is:

$$\left(\frac{\text{Br}}{\text{Cl}}\right) = \frac{{}^{80}\text{Kr}_{\text{Br}}}{{}^{38}\text{Ar}_{\text{Cl}}} \cdot \frac{1}{48.228} \cdot \frac{M_{\text{Br}}}{M_{\text{Cl}}} = \frac{{}^{80}\text{Kr}_{\text{Br}}}{{}^{38}\text{Ar}_{\text{Cl}}} \times 0.04673(\pm 0.00031) \times (\text{wt.ratio}). \quad (13)$$

With $M_{\text{Br}} = 79.904 \pm 0.001$ g/mol, $M_{\text{Cl}} = 35.453 \pm 0.002$ g/mol, $\theta_{79\text{Br}} = 0.5069 \pm 0.0007$, $\theta_{37\text{Cl}} = 0.2424 \pm 0.0010$ (IUPAC periodic

table 2011 <http://www.ciaaw.org/>), $\sigma_{37\text{Cl}} = 0.4330 \pm 0.0060$ b (Pritychenko and Mughabghab, 2012), $\sigma_{79\text{Br}} = 10.89 \pm 0.05$ b (Table 1), $Y_{79\text{Br}} = 0.917$ and $Y_{37\text{Cl}} = 1$.

By comparing the Br/Cl ratio of scapolite to Eq. (13), we can calculate the correction factor:

$$F_{79\text{Br}} = \frac{\text{Br}/\text{Cl}_{\text{Eqn. 13}}}{\text{Br}/\text{Cl}_{\text{scap.}}} \quad (14)$$

In the same way, it is possible to determine $F_{81\text{Br}}$ and F_{I} by using Eqs. (15) and (16),

$$\left(\frac{\text{Br}}{\text{Cl}}\right) = \frac{{}^{82}\text{Kr}_{\text{Br}}}{{}^{38}\text{Ar}_{\text{Cl}}} \times 0.20328(\pm 0.00275)(\text{wt.ratio}) \quad (15)$$

$$\left(\frac{\text{I}}{\text{Cl}}\right) = \frac{{}^{128}\text{Xe}_{\text{I}}}{{}^{38}\text{Ar}_{\text{Cl}}} \times 0.06488(\pm 0.00051)(\text{wt.ratio}). \quad (16)$$

Using halogen ratios is advantageous because it is independent of the sample mass. The correction factor is also independent of the value of the thermal fluence as this term is common to both the sample and standard and cancels out in Eq. (12).

For MN2012b and MN2013a, the scapolite standards were run on the MS1 and ARGUS VI. A small discrepancy exists between Br/Cl and I/Cl values for scapolites from the same irradiation, analysed on different mass spectrometers. Chlorine measurements of scapolite are similar (4.0 ± 0.4 wt.% – MS1 and 4.0 ± 0.3 wt.% – ARGUS VI) on both instruments, thus the discrepancies result from the determination of ${}^{80}\text{Kr}_{\text{Br}}$ and ${}^{128}\text{Xe}_{\text{I}}$. We suggest that the difference is probably related to the measurement procedure. On the ARGUS VI, Xe and Kr isotopes are analysed within 2 min and 4 min respectively following inlet, whereas on the MS1 Xe isotopic analysis does not begin until 12 min after that the gas is admitted into the source of the mass spectrometer, and after 9 min for Kr. Xenon and krypton isotopes are relatively rapidly ionised and depleted in the ion source thus a relatively long delay in measurement could impair the accuracy of extrapolation of data to inlet time into the spectrometer. To establish any effects that the calibration discrepancy may have on sample Br and I determinations, aliquots of six glass MORB samples from the East Pacific Rise (Castillo et al., 2002) were analysed on the MS1 and ARGUS VI mass spectrometers and the noble gas data were used to determine halogen abundances from the scapolite standard data obtained from each spectrometer (Table B.1 in Supplementary data B). The concentrations of Cl, Br and I are plotted in Fig. 4 where the slopes of the linear regressions deviate <5% from the 1:1 line for Cl and I and <15% for Br. Thus it is concluded that samples analysed on different mass spectrometers give consistent data as well as highlighting the importance of analysing standards and samples on the same instrument.

Table 5
Scapolite halogen and potassium data from Kendrick et al. (2013a). Errors are at 2σ .

	BB2/SP	BB1
Cl (wt.%)	4.10 ± 0.15	3.1 ± 0.1
Br (ppm)	40 ± 3	430 ± 30
I (ppb)	50 ± 10	800 ± 130
K (ppm)	9900 ± 170	1200 ± 90
K/Cl	0.23 ± 0.02	0.39 ± 0.03
Br/Cl ($\times 10^{-3}$)	0.97 ± 0.01	13.8 ± 0.8
I/Cl ($\times 10^{-6}$)	1.3 ± 0.3	26 ± 4

Table 6

Average values of noble gas-halogen correction factors calculated using scapolite standards (BB2/SP and BB1) for the four irradiations discussed in this study. FnX values are calculated using Eq. (14), π is calculated using Eq. (10), π^* is the factor for ^{81}Br and ω is calculated using Eq. (11). Uncertainties are given at 1σ and represent the internal precision of each irradiation.

Irradiation	MN2012b				MN2013				MN2014a		MN2014b	
Reactor	Petten								OSU-ICIT		OSU-GRICIT	
Mass-spec	MS1		ARGUS		MS1		ARGUS		ARGUS		ARGUS	
Type	SP/BB2	BB1	SP/BB2	BB1	SP/BB2	BB1	SP/BB2	BB1	SP/BB2	BB1	SP/BB2	BB1
# samp.	7	1	1	0	0	2	3	3	3	5	10	3
π	35.6 ± 2.2	34.5 ± 2.9	28.6 ± 1.2	–	–	35.4 ± 1.0	28.3 ± 1.5	27.2 ± 1.2	50.6 ± 0.7	52.5 ± 2.3	47.1 ± 1.0	46.2 ± 0.6
π^*	10.9 ± 0.6	10.4 ± 0.9	8.5 ± 0.2	–	–	10.8 ± 0.2	8.8 ± 0.4	8.5 ± 0.3	19.2 ± 0.1	20.1 ± 0.8	16.8 ± 0.4	16.5 ± 0.2
ω	29.1 ± 3.6	n.d.	23.3 ± 4.9	–	–	24.4 ± 0.8	26.1 ± 2.3	26.1 ± 1.3	n.d.	64.2 ± 2.0	43.6 ± 2.2	48.0 ± 0.7
$F_{79\text{Br}}$	1.67 ± 0.10	1.63 ± 0.10	1.41 ± 0.06	–	–	1.68 ± 0.05	1.33 ± 0.07	1.29 ± 0.05	2.38 ± 0.03	2.48 ± 0.11	2.21 ± 0.05	2.18 ± 0.03
$F_{81\text{Br}}$	2.22 ± 0.13	2.14 ± 0.12	1.69 ± 0.04	–	–	2.23 ± 0.05	1.80 ± 0.08	1.74 ± 0.06	3.92 ± 0.02	4.13 ± 0.16	3.44 ± 0.09	3.40 ± 0.04
$F_{128\text{I}}$	2.07 ± 0.15	n.d.	1.55 ± 0.14	–	–	1.58 ± 0.05	1.59 ± 0.14	1.69 ± 0.09	n.d.	4.08 ± 0.21	2.66 ± 0.14	3.11 ± 0.05

4.3. Barium calibration

Barium is routinely determined in geological samples, including Mid-Ocean Ridge Basalts (MORB) using a range of analytical techniques including EMP, ICPMS, XRF and ICPEs. Since barium shows strong resonances in neutron absorption at epithermal neutron energies, the ^{131}Xe determinations provide an independent monitor of epithermal fluence in addition to the meteorite and scapolite standards. Barium has the added advantage of being determined in the same sample for which halogens are being measured, which helps to remove any uncertainties associated with neutron flux variations that may exist when using standards located up to a few cm's from a sample's position in an irradiation tube.

Turner (1965) analysed neutron-produced noble gas isotopes from trace elements including Ba. He noted that in meteorites ^{131}Xe is produced by (n, γ , β) reactions from both ^{130}Te and ^{130}Ba . In principle, it is not possible to distinguish between ^{131}Xe produced from Te or Ba unambiguously (Turner, 1965). Meteorites contain relatively high levels of Te and the concentrations Te and Ba are often comparable. However in MORB samples Te shows low abundances of about 3 ± 1 ppb (Yi et al., 2000). In contrast Ba in MORB is consistently above >1 ppm (<http://www.earthchem.org/petdb/>). Thus, the contribution of ^{130}Te to the ^{131}Xe budget in irradiated in MORB samples is considered to be negligible.

^{131}Xe can be produced from neutron induced fission of ^{235}U , we therefore correct ^{131}Xe using $^{134}\text{Xe}_{\text{nf}}$ (Eq. A.25-Supplementary data):

$$^{131}\text{Xe}^* = ^{131}\text{Xe}_{\text{Blk corrected}} - \frac{^{131}\text{Xe}/^{136}\text{Xe}_{\text{nf}}}{^{134}\text{Xe}/^{136}\text{Xe}_{\text{nf}}} \times ^{134}\text{Xe}_{\text{nf}} \quad (17)$$

With $(^{131}\text{Xe}/^{136}\text{Xe})_{\text{nf}} = 0.453 \pm 0.013$ and $(^{134}\text{Xe}/^{136}\text{Xe})_{\text{nf}} = 1.246 \pm 0.036$ (Ozima and Podosek, 2002). This correction accounts for between 1 and 3% of the measured ^{131}Xe in MORB samples.

The Ba abundances are calculated following a similar approach as outlined above for Br (Eq. (9)) by substituting appropriate terms:

$$^{131}\text{Xe}^* = ^{130}\text{Ba} \cdot Y_{130\text{Ba}} \cdot \theta_{130\text{Ba}} \cdot \phi_{\text{th}} \cdot \sigma_{\text{th}} + \phi_{\text{epi}} \cdot \sigma_{\text{epi}} \quad (18)$$

There is uncertainty in the cross section values for Ba in the literature, and epithermal fluence can be up to 23% higher using the values reported by Mughabghab (2006). As a consequence correction factors for Br and I are higher by up to 9% and 13%, respectively, and the sample concentrations of these elements will be therefore underestimated by the same amount. Here the different published cross-sections are reviewed in order to identify the most reasonable value for future studies.

A summary of all the cross section values for ^{130}Ba (n, γ) (published and in web-based compilations) are given in Supplementary data - Table C.4. The National Nuclear Data Center's NUDAT compilation gives a thermal cross-section value of 11.3 ± 1.0 b (<http://www.nndc.bnl.gov>), based on combining the measured values for the production of the ground state (8.8 ± 0.9 b) and the isomeric state (2.5 ± 0.3 b) (Fig. 1). These two measurements were made in 1959 and 1967 respectively using equipment of very low resolution that was perhaps not able to correct for competing decays from the irradiated samples. A compilation by Mughabghab (2006) replaces these values with 7.7 ± 0.9 b and 0.98 ± 0.05 b for ground and isomeric states respectively, giving a combined total cross section of 8.7 ± 0.9 b (<http://www.nndc.bnl.gov/atlas/atlasvalues.html>). The origin of the ground state value is not given by Heft's (1968) measurement using high-resolution Ge detectors. In comparison, Heft's ground state cross section is 6.52 ± 0.40 b.

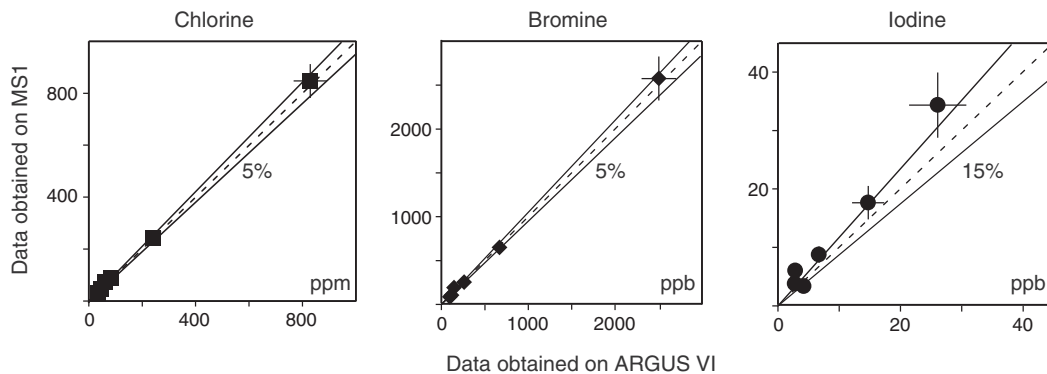


Fig. 4. Halogen concentrations obtained for the same set of MORB samples analysed on the MS1 and ARGUS VI mass spectrometers. The halogen data are corrected using scapolite standards run on each instrument. Chlorine and bromine show a very good agreement (better than 5%). Iodine deviates $<15\%$ from the 1:1 line. Deviations might be caused by sample heterogeneities.

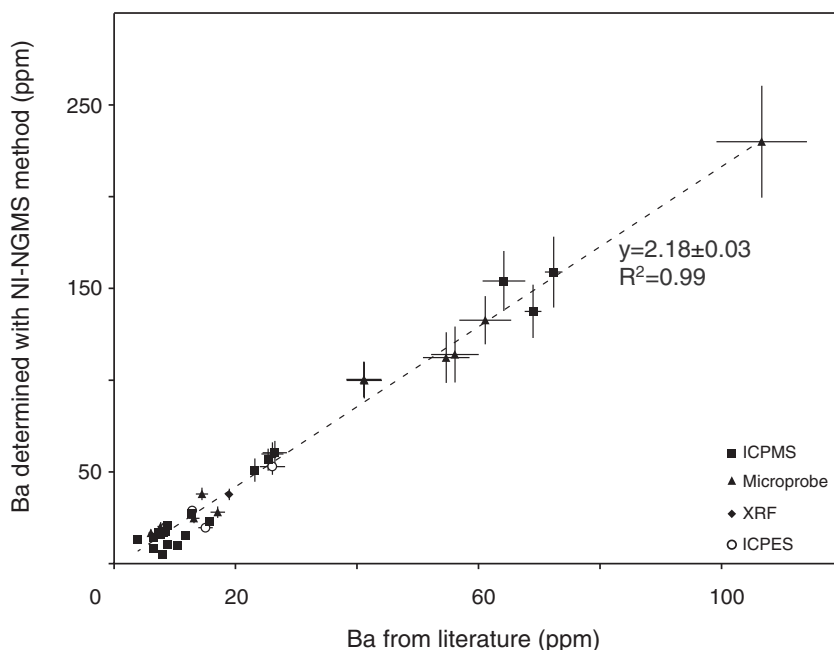


Fig. 5. Barium calibration between MORB literature data (PETdb database) obtained by ICPMS, ICPES, EMP and XRF, and MS1 data in this study. The slope ($F_{130\text{Ba}} = 2.18 \pm 0.03$) demonstrates that 54% of ^{131}Xe is produced by epithermal neutrons during irradiation.

Dauenhauer and Krane (2012) determined the isomeric cross section of 0.596 ± 0.037 b, which differs from Heft's (1968) value due to changes in the accepted value of the gamma-ray branching from the isomeric level. Heft used a then-current value of 40% in his analysis whilst Dauenhauer and Krane (2012) used the now-current value of 55%. If we correct Heft's ground state cross section for the 15% difference of the gamma-ray branching, the isomeric cross section of Dauenhauer and Krane (2012) and (Heft, 1968) would be identical. The ground state cross section of Dauenhauer and Krane (2012) (7.15 ± 0.34 b) is slightly larger than that of Heft (1968) because of their differing values of isomeric cross section. The effects of these corrections somewhat cancel out, so that the total cross section of 7.75 ± 0.34 b (Dauenhauer and Krane, 2012) and 7.48 ± 0.40 b (Heft et al., 1978) overlaps. Both are in substantial disagreement with the value of Mughabghab (2006) based on the early low-resolution measurements. We therefore choose to use the most recent value for the cross-section of ^{130}Ba of 7.75 ± 0.34 b. For the resonant neutron cross section, the value proposed by Dauenhauer and Krane (2012) is 197.3 ± 10.0 b obtained by combining the ground state and the metastable state. This is 11% higher than the

most recent values found in the database of Pritychenko and Mughabghab (2012). This discrepancy remains unexplained although it is possible that the value for the metastable state has not been included in current databases. To maintain consistency, we use the resonant integral data of Dauenhauer and Krane (2012).

During the irradiation MN2012b, 38 MORB and Back-Arc Basin samples (unpublished results) were irradiated for which Ba concentrations have been published (<http://www.earthchem.org/petdb/>). By simply comparing the ^{131}Xe -derived Ba data obtained from the MS1 spectrometer with literature values, without the corrections for the epithermal fluence, a correction factor of 2.18 ± 0.03 (Fig. 5) was obtained. We have calculated the epithermal fluence from the Ba data [$\phi_{\text{epi}} = (2.97 \pm 0.10) \times 10^{17} \text{ n} \cdot \text{cm}^{-2}$] and calculated the correction factors for Br and I using Eq. (23): $F_{79\text{Br}} = 1.55 \pm 0.02$ (1σ), $F_{81\text{Br}} = 1.91 \pm 0.03$ (1σ) and $F_{127\text{I}} = 2.16 \pm 0.04$ (1σ).

We use this new set of factors to correct the six MORB data (Castillo et al., 2002) and compare the final results to the ones obtained using the scapolite standards (Fig. 6 and Table B.1-Supplementary data section B). For bromine the barium-based calibration slightly overestimates the

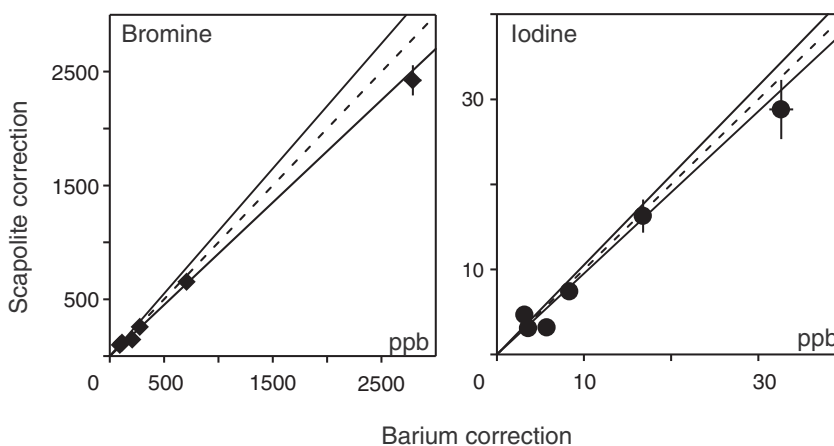


Fig. 6. Comparison of the calibration of bromine and iodine concentrations using neutron fluences derived from barium versus direct calibration using scapolite standards. We show the 1:1 line with an envelope of 10% error for bromine and 5% error for iodine. Error bar is 1σ .

Table 7ARe-determination of I/Cl ratio in BB2/SP standards. The calculated value is 8.5% lower than the value calculated by Kendrick et al. (2013a) and the error bar is reduced from 23% to 14% (2 σ).

Irradiation	Mass-spect.	Correction	Sample name	I/Cl (10^{-6})	\pm (1 σ)
MN2012	MS1	Barium	BB2_1	1.34	0.13
	MS1	Barium	BB2_2	1.26	0.11
	MS1	Barium	BB2_3	1.27	0.09
	MS1	Barium	BB2_4	1.16	0.08
	MS1	Barium	BB2_5	1.16	0.09
	MS1	Barium	BB2_6	1.20	0.10
	MS1	Barium	BB2_7	1.39	0.16
	ARGUS VI	SW-MN2012f	BB2_8	1.20	0.08
MN2013	ARGUS VI	SW-step heating	BB2_9	1.17	0.12
	ARGUS VI	SW-step heating	BB2_10	1.18	0.12
	ARGUS VI	SW-step heating	BB2_11	1.30	0.12
	ARGUS VI	SW-step heating	BB2_12	1.08	0.07
MN2014b	ARGUS VI	SW-step heating	BB2_13	1.24	0.08
	ARGUS VI	SW-step heating	BB2_14	1.12	0.07
	ARGUS VI	SW-step heating	BB2_15	1.05	0.07
	ARGUS VI	SW-step heating	BB2_16	1.14	0.07
	ARGUS VI	SW-step heating	BB2_17	1.18	0.08
	ARGUS VI	SW-step heating	BB2_18	1.16	0.07
	ARGUS VI	SW-step heating	BB2_19	1.08	0.07
	ARGUS VI	SW-step heating	BB2_20	1.10	0.07
	ARGUS VI	SW-step heating	BB2_21	1.19	0.08
	Average (+ stdev)			1.19	0.09
	Average (+ s.e.m.)			1.19	0.02

abundances by 7.4%. In contrast the difference between barium and scapolite calibrations for I is <5%. We attribute this variation to the contrast in thermal/epithermal neutron cross sections (Q_0) for target elements involved. Using the data in Table 1, Q_0 values are very similar for ^{127}I and ^{130}Ba at 24.9 ± 0.7 and 25.5 ± 1.7 respectively, whereas ^{80}Br has a much lower Q_0 of only 11.9 ± 0.3 . Therefore, $^{128}\text{Xe}/\text{I}$ and $^{131}\text{Xe}/\text{Ba}$ production rates should be similar and largely independent of the neutron energy distribution of the irradiation.

5. Cross-calibration of I/Cl ratio in scapolites (BB2/SP and BB1)

The scapolite Br and I abundances of Kendrick (2012) were subsequently revised by 22% and 27% respectively by Kendrick et al. (2013a). The authors attributed the revision to irradiation of samples in a strongly thermalized neutron flux, therefore negating the requirement to estimate the epithermal neutron contribution via inclusion of a meteorite standard. Bromine concentrations were subsequently confirmed using LA-ICPMS (Hammerli et al., 2014), whereas the I abundances in scapolites have not been cross-calibrated using an independent iodine standard.

The Shallowater aubrite step heating data, as well as the Ba correction, are used here to re-evaluate the I/Cl ratio for SP/BB2 ($n = 21$) and for BB1 ($n = 10$) standards irradiated between 2012 and 2014 (Tables 7A and 7B and Fig. 7).

Based on this, the new recommended I/Cl values are 1.19×10^{-6} (s.t.d. $\pm 0.09\text{-}1\sigma$ or s.e.m. $\pm 0.02\text{-}1\sigma$) for BB2/SP and 25.9×10^{-6} for BB1 (s.t.d. $\pm 1.3\text{-}1\sigma$ or s.e.m. $\pm 0.4\text{-}1\sigma$).

This brings BB1 and SP/BB2 scapolite standards to the same level of certainty as SY scapolites, not measured in that study. Despite this improvement, it seems clear that the correction based on Shallowater aubrite or the barium correction produce smaller errors as shown in the Supplementary data (Table B1) for the ALARCON set of samples.

6. Conclusion

The main findings of this study are summarised as follows.

- 1) We provide details of the analytical procedures for obtaining Ar, Kr and Xe isotope determinations using the ARGUS VI multicollector noble gas mass spectrometer. We compare the data obtained with our existing MS1 mass spectrometer to demonstrate the improvement in performance and data quality of the multicollector instrument.
- 2) The general principles and data reduction procedures are described in detail for the conversion of halogen-derived noble gas isotopes to halogen abundances. We show that the use of standards of known concentrations of each element is preferred, over direct calculation based on neutron flux determinations.

Table 7BRe-determination of I/Cl ratio in BB1 standards. The calculated value is the same as the value calculated by Kendrick et al. (2013a,b) and the error bar is reduced from 15% to 10% (2 σ).

Irradiation	Mass-spect.	Correction	Sample name	I/Cl (10^{-6} wt.)	\pm (1 σ)
MN2013	ARGUS VI	SW-step heating	BB1_1	27.3	2.6
	ARGUS VI	SW-step heating	BB1_2	28.0	2.6
	ARGUS VI	SW-step heating	BB1_3	25.4	2.7
MN2014a	ARGUS VI	SW-step heating	BB1_4	23.8	1.0
	ARGUS VI	SW-step heating	BB1_5	24.8	1.0
	ARGUS VI	SW-step heating	BB1_6	25.7	1.0
	ARGUS VI	SW-step heating	BB1_7	25.0	1.0
MN2014b	ARGUS VI	SW-step heating	BB1_8	26.9	1.7
	ARGUS VI	SW-step heating	BB1_9	26.1	1.7
	ARGUS VI	SW-step heating	BB1_10	26.6	1.7
Average (+ stdev)				25.9	1.3
Average (+ s.e.m.)				25.9	0.4

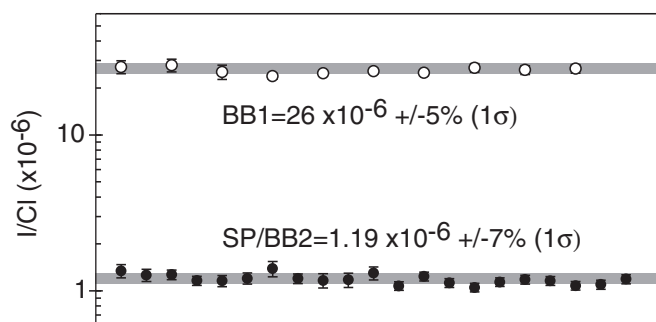


Fig. 7. Scapolite standards used to monitor the production of $^{38}\text{Ar}_{\text{Cl}}$, $^{80}\text{Kr}_{\text{Br}}$ and $^{128}\text{Xe}_{\text{I}}$ in four irradiations have good reproducibility. The absolute I/Cl ratios recommended for the standards have been revised using a combination of techniques described in this study.

- 3) Step-heating of Shallowwater meteorite standard is recommended to generate a correlation line on a plot of $^{129}\text{Xe}/^{132}\text{Xe}$ vs. $^{128}\text{Xe}/^{132}\text{Xe}$ and to obtain the $^{128}\text{Xe}/^{127}\text{I}$ ratio for an irradiation.
- 4) A barium calibration, which is completely independent of other standards, shows excellent agreement with both Shallowwater and the newly revised I/Cl ratio for scapolite standards for the determination of iodine. This correction can be used as an internal standard within each irradiation if Ba contents have been independently determined.
- 5) Scapolite standards are a very good standard for bromine and can also be used as an iodine standard, however we recommend to use Shallowwater aubrite or the barium calibration for iodine. The value of I/Cl ratio for BB2/SP scapolite has been revised downward by 8.5%. The new recommended value for BB2/SP is $(1.19 \pm 0.09) \times 10^{-6}$ (1σ). For BB1, we recommend a I/Cl ratio of $(25.9 \pm 1.3) \times 10^{-6}$ (1σ).

List of the constants

Name	Value	Error	Unit	Reference
$^{40}\text{Ar}/^{36}\text{Ar}$	298.56	0.31	–	Lee et al. (2006)
$^{38}\text{Ar}/^{36}\text{Ar}$	0.1880	–	–	Ozima and Podosek (2002)
t_{Hb3gr}	1074.9	3.5	Ma	Schwarz and Trierloff (2007)
λ_e	0.576×10^{-10}	0.002×10^{-10}	a^{-1}	This study (Table A.2. Supp. Data)
λ_β	4.955×10^{-10}	0.013×10^{-10}	a^{-1}	This study (Table A.2. Supp. Data)
λ_{tot}	5.531×10^{-10}	0.013×10^{-10}	a^{-1}	This study (Table A.2. Supp. Data)
K_{Hb3gr}	1.247	0.008	wt. %	Roddick (1983)
Ca_{Hb3gr}	7.45	0.05	wt. %	Roddick (1983)
Cl_{Hb3gr}	0.283	0.002	wt. %	Roddick (1983)
M_{Ca}	40.078	0.004	$\text{g} \cdot \text{mol}^{-1}$	IUPAC (2013)
M_{K}	39.0983	0.00001	$\text{g} \cdot \text{mol}^{-1}$	IUPAC (2013)
M_{Cl}	35.453	0.0002	$\text{g} \cdot \text{mol}^{-1}$	IUPAC (2013)
M_{I}	126.90447	0.00003	$\text{g} \cdot \text{mol}^{-1}$	IUPAC (2013)
M_{Br}	79.904	0.001	$\text{g} \cdot \text{mol}^{-1}$	IUPAC (2013)
M_{Ba}	137.327	0.007	$\text{g} \cdot \text{mol}^{-1}$	IUPAC (2013)
$^{40}\text{K}/\text{K}$	1.17×10^{-4}	0.01×10^{-4}	–	IUPAC (2013)
$^{37}\text{Cl}/\text{Cl}$	0.2424	0.0010	–	IUPAC (2013)
$^{79}\text{Br}/\text{Br}$	0.5069	0.0007	–	IUPAC (2013)
$^{81}\text{Br}/\text{Br}$	0.4931	0.0007	–	IUPAC (2013)
$^{130}\text{Ba}/\text{Ba}$	0.00106	0.0001	–	IUPAC (2013)
$\gamma_{^{136}\text{Xe}}$	6.47	0.47	%	Ozima and Podosek (2002)
$\gamma_{^{86}\text{Kr}}$	2.04	0.02	%	Ozima and Podosek (2002)
$(^{134}\text{Xe}/^{136}\text{Xe})_{\text{nf}}$	1.246	0.036	–	Ozima and Podosek (2002)
$(^{84}\text{Kr}/^{86}\text{Kr})_{\text{nf}}$	0.50	0.02	–	Ozima and Podosek (2002)
$(^{131}\text{Xe}/^{136}\text{Xe})_{\text{nf}}$	0.453	0.013	–	Ozima and Podosek (2002)
$(^{80}\text{Kr}/^{84}\text{Kr})_{\text{air}}$	0.03960	0.00002	–	Ozima and Podosek (2002)
$(^{129}\text{Xe}/\text{I})_0$	1.072×10^{-4}	0.029×10^{-4}	–	Brazzle et al. (1999)

Acknowledgements

We dedicate this work to the memory of our friend and colleague, Dr. Pete Burnard (CRPG-Nancy), who worked at the University of Manchester from 1987–1998.

We thank Dr. D. Chavrit for providing some back arc basalt barium data used in this paper. We are grateful to Dr. S. Crowther, who provided the data of Shallowwater run on RELAX for the irradiations MN2012f and MN2014a. We thank Dave Hilton who provided the Alarcon samples. We would like to thank Doug Hamilton (ThermoFisher Scientific) for advice on achieving Kr and Xe measurements on the ARGUS VI. We thank Jamie Gilmour for helpful insights and suggestion that improved the manuscript. Mark Kendrick and Hirochika Sumino are thanked for thorough reviews and suggestions that led to a much improved, more succinct manuscript.

This work was performed in the framework of the “NOBLE” (The Origin, Accretion and Differentiation of Extreme Volatiles in Terrestrial Planets) research project and funded by the European Research Council (ERC) grant No: 267692 under the European Commission Seventh Framework Programme (FP7). The ARGUS VI mass spectrometer is funded by Science and Technology Facilities Council grants ST/M001253/1/1 and ST/L002957/1 (UKCAN) at the University of Manchester.

Appendix A. Supplementary data

Supplementary data to this article can be found online at <http://dx.doi.org/10.1016/j.chemgeo.2016.05.003>.

References

- Ballentine, C.J., Burgess, R., Marty, B., 2002. Tracing fluid origin, transport and interaction in the crust. *Rev. Mineral. Geochem.* 47, 539–614.
- Böhlke, J.K., Irwin, J.J., 1992a. Laser microprobe analyses of Cl, Br, I and K in fluids inclusions: implications for sources of salinity in some ancient hydrothermal fluids. *Geochim. Cosmochim. Acta* 56, 203–225.
- Böhlke, J.K., Irwin, J.J., 1992b. Laser microprobe analyses of noble gas isotopes and halogens in fluid inclusions: analyses of microstandards and synthetic inclusion in quartz. *Geochim. Cosmochim. Acta* 56, 187–201.
- Bottrell, S.H., Yardley, B.W.D., 1988. The composition of a primary granite-derived ore fluid from S.W. England, determined by fluid inclusion analysis. *Geochim. Cosmochim. Acta* 52, 585–588.
- Brazzle, R.H., Pravdivtseva, O.V., Meshik, A.P., Hohenberg, C.M., 1999. Verification and interpretation of the I-Xe chronometer. *Geochim. Cosmochim. Acta* 63, 739–760.
- Burgess, R., Layzelle, E., Turner, G., Harris, J.W., 2002. Constraints on the age and halogen composition of mantle fluids in Siberian coated diamonds. *Earth Planet. Sci. Lett.* 197, 193–203.
- Burgess, R., Cartigny, P., Harrison, D., Hobson, E., Harris, J., 2009. Volatile composition of microinclusions in diamonds from the Panda kimberlite, Canada: implications for chemical and isotopic heterogeneity in the mantle. *Geochim. Cosmochim. Acta* 73, 1779–1794.
- Castillo, P.R., Yardley, B.W.D., Lonsdale, P.F., Hilton, D.R., Shaw, A.M., Glascock, M.D., 2002. Petrology of Alarcon Rise lavas, Gulf of California: nascent intracontinental ocean crust. *J. Geophys. Res. Solid Earth* 107 ECV 5-1–ECV 5-15.
- Chilian, C., St-Pierre, J., Kennedy, G., 2006. Dependence of thermal and epithermal neutron self-shielding on sample size and irradiation site. *Nucl. Inst. Methods Phys. Res. A* 564, 629–635.
- Chilian, C., St-Pierre, J., Kennedy, G., 2008. Complete thermal and epithermal neutron self-shielding corrections for NAA using a spreadsheet. *J. Radioanal. Nucl. Chem.* 278, 745–749.
- Chilian, C., Chambon, R., Kennedy, G., 2010. Neutron self-shielding with k0-NAA irradiations. *Nucl. Inst. Methods Phys. Res. A* 622, 429–432.
- Crowther, S.A., Mohapatra, R.K., Turner, G., Blagburn, D.J., Kehm, K., Gilmour, J.D., 2008. Characteristics and applications of RELAX, an ultrasensitive resonance ionization mass spectrometer for xenon. *J. Anal. At. Spectrom.* 23, 938–947.
- Dauenhauer, A.Y., Krane, K.S., 2012. Neutron capture cross section of ^{130}Ba , ^{132}Ba , ^{134}Ba , ^{136}Ba . *Phys. Rev. C* 85.
- Gilmour, J.D., Hewett, S.M., Lyon, I.C., Stringer, M., Turner, G., 1991. A resonance ionization mass spectrometer for xenon. *Meas. Sci. Technol.* 2, 589.
- Gilmour, J.D., Lyon, I.C., Johnston, W.A., Turner, G., 1994. RELAX: an ultrasensitive, resonance ionization mass spectrometer for xenon. *Rev. Sci. Instrum.* 65, 617–625.
- Gilmour, J.D., Pravdivtseva, O.V., Busfield, A., Hohenberg, C.M., 2006. The I-Xe chronometer and the early solar system. *Meteorit. Planet. Sci.* 41, 19–31.
- Hammerli, J., Rusk, B., Spandler, C., Emsbo, P., Oliver, N.H.S., 2013. In situ quantification of Br and Cl in minerals and fluid inclusions by LA-ICP-MS: a powerful tool to identify fluid sources. *Chem. Geol.* 337, 338, 75–87.

- Hammerli, J., Spandler, C., Oliver, N.H.S., Rusk, B., 2014. Cl/Br of scapolite as a fluid tracer in the earth's crust: insights into fluid sources in the Mary Kathleen Fold Belt, Mt. Isa Inlier, Australia. *J. Metamorph. Geol.* 32, 93–112.
- Heft, R.E., 1968. In Conference on Computers in Activation Analysis. edited by R. Farmakes (American Nuclear Society, La Grange Park, IL, 1968).
- Heft, R.E., 1978. A consistent set of nuclear-parameter values for absolute INAA. In: Farmakes, R. (Ed.), *Proceedings of the Conference on Computers in Activation Analysis*. American Nuclear Society, La Grange Park, pp. 495–510.
- Heinrich, C.A., Bain, J.H.C., Fardy, J.J., Waring, C.L., 1993. Br/Cl geochemistry of hydrothermal brines associated with Proterozoic metasediment-hosted copper mineralization at Mount Isa, northern Australia. *Geochim. Cosmochim. Acta* 57, 2991–3000.
- Heinrich, C.A., Pettke, T., Halter, W.E., Aigner-Torres, M., Audotat, A., Gunther, D., Hattendorf, B., Bleiner, D., Guillon, M., Horn, I., 2003. Quantitative multi-element analysis of minerals, fluid and melt inclusions by laser-ablation inductively-coupled-plasma mass-spectrometry. *Geochim. Cosmochim. Acta* 67, 3473–3497.
- Hohenberg, C.M., 1967. I-Xe dating of the shallowwater achondrite. *Earth Planet. Sci. Lett.* 3, 357–362.
- Hohenberg, C.M., Kennedy, B.M., 1981. I-Xe dating: intercomparisons of neutron irradiations and reproducibility of the Bjurböle standards. *Geochim. Cosmochim. Acta* 45, 251–256.
- Irwin, J.J., Roedder, E., 1995. Diverse origins of fluids in magmatic inclusions at Bingham (Utah, USA), Butte (Montana, USA), St Austell (Cornwall, UK) and Ascension Island (mid-Atlantic, UK) indicated by laser microprobe analysis of Cl, K, Br, I, Ba + Te, U, Ar, Kr and Xe. *Geochim. Cosmochim. Acta* 59, 295–312.
- Joachim, B., Pawley, A., Lyon, I.C., Marquardt, K., Henkel, T., Clay, P.L., Ruzié, L., Burgess, R., Ballentine, C.J., 2015. Experimental partitioning of F and Cl between olivine, orthopyroxene and silicate melt at Earth's mantle conditions. *Chem. Geol.* 416, 65–78.
- Johnson, L.H., Burgess, R., Turner, G., Milledge, H.J., Harris, J.W., 2000. Noble gas and halogen geochemistry of mantle fluids: comparison of African and Canadian diamonds. *Geochim. Cosmochim. Acta* 64, 717–732.
- Kelley, S., Turner, G., Butterfield, A.W., Shepherd, T.J., 1986. The source and significance of argon isotopes in fluid inclusions from areas of mineralization. *Earth Planet. Sci. Lett.* 79, 303–318.
- Kendrick, M.A., 2012. High precision Cl, Br and I determinations in mineral standards using the noble gas method. *Chem. Geol.* 292, 293, 116–126.
- Kendrick, M.A., Burnard, P., 2013. Noble gases and halogens in fluid inclusions: a journey through the Earth's crust. In: Burnard, P. (Ed.), *The Noble Gases as Geochemical Tracers*. Springer-Verlag, Berlin Heidelberg, p. 391.
- Kendrick, M.A., Burgess, R., Pattick, R.A.D., Turner, G., 2001. Halogen and Ar-Ar age determinations of inclusions within quartz veins from porphyry copper deposits using complementary noble gas extraction techniques. *Chem. Geol.* 177, 351–370.
- Kendrick, M.A., Scambelluri, M., Honda, M., Phillips, D., 2011. High abundances of noble gas and chlorine delivered to the mantle by serpentinite subduction. *Nat. Geosci.* 4, 807–812.
- Kendrick, M.A., Kamenetsky, V.S., Phillips, D., Honda, M., 2012a. Halogen systematics (Cl, Br, I) in Mid-Ocean Ridge Basalts: a Macquarie Island case study. *Geochim. Cosmochim. Acta* 81, 82–93.
- Kendrick, M.A., Woodhead, J.D., Kamenetsky, V.S., 2012b. Tracking halogens through the subduction cycle. *Geology* 40, 1075–1078.
- Kendrick, M.A., Arculus, R.J., Burnard, P., Honda, M., 2013a. Quantifying brine assimilation by submarine magmas: examples from the Galapagos Spreading Centre and Lau Basin. *Geochim. Cosmochim. Acta* 123, 150–165.
- Kendrick, M.A., Honda, M., Pettke, T., Scambelluri, M., Phillips, D., Guilian, A., 2013b. Subduction zone fluxes of halogens and noble gases in seafloor and forearc serpentinites. *Earth Planet. Sci. Lett.* 365, 86–96.
- Kusebauch, C., John, T., Whitehouse, M.J., Klemme, S., Putnis, A., 2015. Distribution of halogens between fluid and apatite during fluid-mediated replacement processes. *Geochim. Cosmochim. Acta* 170, 225–246.
- Lee, J.Y., Marti, K., Severinghaus, J.P., Kawamura, K., Yoo, H.S., Lee, J.B., Kim, J.S., 2006. A re-determination of the isotopic abundances of atmospheric Ar. *Geochimica et Cosmochimica Acta* 70, 4507–4512.
- Ludwig, K.R., 2012. *Isoplot, A Geochronological Toolkit for Microsoft Excel*. Berkeley Geochronology Center, Special Publication No. 5 p. 75.
- McDougall, I., Harrison, T.M., 1999. *Geochronology and Thermochronology by the $^{40}\text{Ar}/^{39}\text{Ar}$ Method*. Oxford University Press, Oxford.
- Merrihue, C.M., 1965. Trace element determinations and potassium-argon dating by mass spectrometry of neutron-irradiated samples. *Trans. Am. Geophys. Union* 125.
- Mughabghab, S.F., 2006. *Atlas of Neutron Resonances, Resonance Parameters and Neutron Cross Sections Z = 1–100*. Elsevier, Amsterdam.
- Ozima, M., Podosek, F.A., 2002. *Noble Gas Geochemistry*, second ed. Cambridge University Press, New York.
- Pritychenko, B., Mughabghab, S.F., 2012. Neutron thermal cross sections, Westcott factors, resonance integrals, Maxwellian averaged cross sections and astrophysical reaction rates calculated from the ENDF/B-VII.1, JEFF-3.1.2, JENDL-4.0, ROSFOND-2010, CENDL-3.1 and EAF-2010 evaluated data libraries. *Nucl. Data Sheets* 113, 3120–3144.
- Pure and Applied Chemistry, April 2013. (ISSN: 1365-3075, 0033-4545) 85 (5), 1047–1078. <http://dx.doi.org/10.1351/PAC-REP-13-03-02>.
- Roddick, J.C., 1983. High precision intercalibration of ^{40}Ar – ^{39}Ar standards. *Geochim. Cosmochim. Acta* 47, 887–898.
- Schwarz, W.H., Trierloff, M., 2007. Intercalibration of ^{40}Ar – ^{39}Ar age standards NL-25, HB3gr hornblende, GA1550, SB-3, HD-B1 biotite and BMus/2 muscovite. *Chem. Geol.* 242, 218–231.
- Sumino, H., Burgess, R., Mizukami, T., Wallis, S.R., Holland, G., Ballentine, C.J., 2010. Seawater-derived noble gases and halogens preserved in exhumed mantle wedge peridotite. *Earth Planet. Sci. Lett.* 294, 163–172.
- Turner, G., 1965. Extinct iodine 129 and trace elements in chondrite. *J. Geophys. Res.* 70, 5433–5445.
- Turner, G., 1972. ^{40}Ar – ^{39}Ar age and irradiation history of the Apollo 15 anorthosite, 15415. *Earth Planet. Sci. Lett.* 14, 169–175.
- Turner, G., Bannon, M.P., 1992. Argon isotope geochemistry of inclusion fluids from granite-associated mineral veins in southwest and northeast England. *Geochim. Cosmochim. Acta* 56, 227–243.
- Turner, G., Huneke, J.C., Podosek, F.A., Wasserburg, G.J., 1971. ^{40}Ar – ^{39}Ar ages and cosmic ray exposure ages of Apollo 14 samples. *Earth Planet. Sci. Lett.* 12, 19–35.
- Yi, W., Halliday, A.N., Alt, J.C., Lee, D.-C., Rehkämper, M., Garcia, M.O., Langmuir, C.H., Su, Y., 2000. Cadmium, indium, tin, tellurium, and sulfur in oceanic basalts: implications for chalcophile element fractionation in the earth. *J. Geophys. Res. Solid Earth* 105, 18927–18948.